Experimental Analysis of the Antibonding Trimetal Character of the HOMO in the Paramagnetic Fischer-Palm $Ni_3(\eta^5\text{-}C_5H_5)_3(\mu_3\text{-}CO)_2$ Cluster: Synthesis and Stereochemical Characterization of the Electronically Equivalent $[(\eta^5\text{-}C_5Me_5)CoNi_2(\eta^5\text{-}C_5H_5)_2(\mu_3\text{-}CO)_2]^-$ Monoanion and Neutral $Ni_3(\eta^5\text{-}C_5Me_5)_3(\mu_3\text{-}CO)_2$ Analogue and of the $[Ni_3(\eta^5\text{-}C_5H_5)_3(\mu_3\text{-}CO)_2]^-$ Monoanion

Joseph J. Maj,[1a] A. David Rae,[1b] and Lawrence F. Dahl*

Contribution from the Department of Chemistry, University of Wisconsin—Madison, Madison, Wisconsin 53706. *Received August 24, 1981*

Abstract: The preparation and characterization by X-ray diffraction and other physical methods are reported for three triangular metal cyclopentadienyl carbonyl clusters, viz., the monoanion (**2**), isolated as the $[K(2,2,2\text{-crypt})]^+$ salt, from the one-electron reduction of $(\eta^5\text{-}C_5Me_5)CoNi_2(\eta^5\text{-}C_5H_5)_2(\mu_3\text{-}CO)_2$ (**1**) with potassium naphthalenide, the monoanion (**4**), isolated as the $[K(2,2,2\text{-crypt})]^+$ salt, from the one-electron reduction of the Fischer-Palm (FP) $Ni_3(\eta^5\text{-}C_5H_5)_3(\mu_3\text{-}CO)_2$ (**3**) with potassium acenaphthalenide, and $Ni_3(\eta^5\text{-}C_5Me_5)_3(\mu_3\text{-}CO)_2$ (**5**), produced by the photochemical reaction of $Ni_2(\eta^5\text{-}C_5Me_5)_2(\mu_2\text{-}CO)_2$ and nickelocene. Comparative structural features of the monoanions **2** and **4** provide unambiguous experimental evidence for the Strouse-Dahl bonding model (1969), which postulated that the HOMO in the classical FP molecule **3** is primarily an in-plane, trimetal antibonding orbital of nondegenerate a_2' representation under D_{3h} symmetry. The most notable structural difference upon the formation of **2** from **1**, both of whose central $CoNi_2(CO)_2$ cores closely conform to C_{2v}—2*mm* symmetry, is that the Ni-Ni bond in the paramagnetic monoanion has enlarged by 0.062 Å from 2.326 (2) Å in **1** to 2.388 (2) Å in **2** relative to the smaller but significant increase in the two equivalent Co-Ni bonds by 0.021 Å from 2.371 Å in **1** to 2.392 Å in **2**. These bond-length increases reflect the addition of the unpaired electron in **2** to an antibonding trimetal MO which for the $CoNi_2$ cluster has substantially greater Ni 3d AO than Co 3d AO character. The resulting mean of 2.390 Å for the virtually identical Co-Ni and Ni-Ni bond lengths in **2** is experimentally the same as that of 2.389 (2) Å found for the three crystallographically identical Ni-Ni bond lengths in the electronically equivalent **3**. The observation that the monoanion **4** has an average Ni-Ni bond length of 2.421 Å, which is 0.032 Å larger than that in the neutral FP parent **3**, provides further proof for the trimetal antibonding character of the HOMO containing one electron in **3** and two electrons in **4**; its nondegeneracy is conclusively demonstrated from magnetic susceptibility measurements which show **4** to be diamagnetic at room temperature. The slight observed distortion in the $Ni_3(CO)_2$ core of **4** from a regular D_{3h} configuration toward C_s-σ_v symmetry may be attributed to electronic considerations, by which the HOMO of **4** can thereby acquire carbonyl character which is symmetry forbidden for the HOMO of **3** under threefold rotational site symmetry. The structural determination and refinement of **5**, an unprecedented example (to our knowledge) of a triangularly bonded metal cluster with three pentamethylcyclopentadienyl ligands, were complicated by a crystal-twinning problem, which was overcome by the use of the least-squares program RAELS. This permethylated analogue of **3** possesses crystallographic C_{3h}—3/*m* site symmetry for a single-crystal component of a twinned lattice; the central $Ni_3(CO)_2$ core of **5** conforms to D_{3h} symmetry. An examination reveals that the replacement of three C_5H_5 rings in **3** with three sterically bulky C_5Me_5 rings in **5** causes a marked lengthening of the Ni-Ni bond lengths by 0.14 Å, which with essentially no increase in the Ni-C(ring) distances emphasizes the relative weakness of the metal-metal bonds. The fact that cyclic voltammetric measurements of the neutral permethylated derivative **5** display two reversible oxidation waves in addition to a reversible reduction wave is consistent with the premise that the inherent stability of the FP molecule **3** under strong oxidizing conditions is a consequence of a charge effect involving enhanced $d\pi(Ni) \rightarrow \pi^*(CO)$ back-bonding dominating over the destabilizing effect of the trinickel antibonding a_2' HOMO being occupied by one electron in **3** or two electrons in **4**.

Systematic studies of the geometrical effects caused by the addition or removal of valence electrons have been essential in elucidating the nature of metal-metal bonds in a variety of metal cluster systems,[2] many of which function as electron-transfer reagents without breakdown of the central cluster framework. This research, which has been pedagogically denoted[3] as "experimental quantum mechanics", has involved the construction from stereochemical analysis of qualitative metal cluster correlation diagrams whose energy-level ordering is dictated by the nature and number of ligands attached to the central cluster core. These structural-bonding considerations not only have been utilized in correlating and predicting alterations in geometry with changes in electronic configurations but also have proven highly useful in rationalizing the observed variations in physicochemical properties and chemical reactions of metal clusters containing a common metal-core architecture (e.g., a cubane-like Fe_4S_4 core) to which different terminal ligands are coordinated.[4-7]

(1) (a) Based in part on the Ph.D. thesis of J. J. Maj at the University of Wisconsin—Madison, 1981. (b) On leave (December 1979-June, 1980) at UW—Madison from School of Chemistry, University of New South Wales, Kensington, New South Wales 2033, Australia.

(2) (a) Ginsburg, R. E.; Rothrock, R. K.; Finke, R. G.; Collman, J. P.; Dahl, L. F. *J. Am. Chem. Soc.* **1979**, *101*, 6550-6562 and references therein. (b) Simon, G. L.; Dahl, L. F. *Ibid.* **1973**, *95*, 2164-2174 and references therein. (c) Lemmen, T. H.; Kocal, J. A.; Lo, F. Y.-K.; Chen, M. W.; Dahl, L. F. *Ibid.* **1981**, *103*, 1932-1941 and references therein. (d) Paquette, M. S.; Dahl, L. F. *Ibid.* **1980**, *102*, 6621-6623.

(3) Fenske, R. F., private communication to L. F. Dahl.

(4) (a) Wei, C. H.; Wilkes, G. R.; Treichel, P. M.; Dahl, L. F. *Inorg. Chem.* **1966**, *5*, 900-905. (b) Schunn, R. A.; Fritchie, C. J., Jr.; Prewitt, C. T. *Ibid.* **1966**, *5*, 892-899. (c) Trinh-Toan; Fehlhammer, W. P.; Dahl, L. F. *J. Am. Chem. Soc.* **1977**, *99*, 402-407. (d) Trinh-Toan; Teo, B. K.; Ferguson, J. A.; Meyer, T. J.; Dahl, L. F. *Ibid.* **1977**, *99*, 408-416.

(5) (a) Averill, B. A.; Herskovitz, T.; Holm, R. H.; Ibers, J. A. *J. Am. Chem. Soc.* **1973**, *95*, 3523-3534. (b) Que, L., Jr.; Bobrick, M. A.; Ibers, J. A.; Holm, R. H. *Ibid.* **1974**, *96*, 4168-4178. (c) Carrell, M. C.; Glusker, J. P.; Job, R.; Bruice, T. C. *Ibid.* **1977**, *99*, 3683-3690. (d) Laskowski, E. J.; Frankel, R. B.; Gillum, W. O.; Papaefthymiou, G. C.; Renaud, J.; Ibers, J. A.; Holm, R. H. *Ibid.* **1978**, *100*, 5322-5337. (e) Laskowski, E. J.; Reynolds, J. G.; Frankel, R. B.; Foner, S.; Papaefthymiou, G. C.; Holm, R. H. *Ibid.* **1979**, *101*, 6552-6570. (f) Berg. J. M. Hodgson, K. O.; Holm, R. H. *Ibid.* **1979**, *101*, 4586-4593. (g) Bobrik, M. A.; Hodgson, K. O.; Holm, R. H. *Inorg. Chem.* **1977**, *16*, 1851-1858. (h) Ibers, J. A.; Holm, R. H. *Science* (Washington, D. C.) **1980**, 209, 223-235 and references therein.

(6) (a) Gall, R. S.; Chu, C. T.-W.; Dahl, L. F. *J. Am. Chem. Soc.* **1974**, *96*, 4019-4023. (b) Chu, C. T.-W.; Lo, F. Y.-K.; Dahl, L. F. *J. Am. Chem. Soc.*, in press.

0002-7863/82/1504-3054$01.25/0

Such studies of the classical Fischer–Palm $Ni_3(\eta^5\text{-}C_5H_5)_3(\mu_3\text{-}CO)_2$ molecule[8] and its structural analogues[9] have been directed toward an experimental characterization of the type (and symmetry properties) of the HOMO containing the unpaired electron in the trinickel cluster. We also hoped to uncover an explanation as to why several attempts in our laboratory to remove this unpaired electron by oxidation to the monocation were unsuccessful. A formal removal of the unpaired electron in $Ni_3(\eta^5\text{-}C_5H_5)_3(\mu_3\text{-}CO)_2$ was accomplished[10] by the replacement of one nickel atom with a cobalt atom that was also labeled with a pentamethylcyclopentadienyl ligand (in order to provide a crystal-ordered molecule). A comparative geometrical analysis with the Fischer–Palm trinickel molecule of both the resulting diamagnetic, crystal-disordered $CoNi_2(\eta^5\text{-}C_5H_5)_3(\mu_3\text{-}CO)_2$, which is isomorphous[11] with $Ni_3(\eta^5\text{-}C_5H_5)_3(\mu_3\text{-}CO)_2$ in the crystalline state, and the corresponding crystal-ordered $(\eta^5\text{-}C_5Me_5)CoNi_2(\eta^5\text{-}C_5H_5)_2(\mu_3\text{-}CO)_2$ revealed virtually identical decreases in the average metal–metal distance of 0.031 and 0.033 Å, respectively. This significant bond-length shortening was viewed to be the consequence of the unpaired electron in the Fischer–Palm molecule residing in a HOMO with highly antibonding trinickel character, in accordance with the proposed Strouse–Dahl antibonding in-plane trimetal a_2' HOMO model[12] (under D_{3h} symmetry) as opposed to the originally formulated Longuet-Higgins–Stone bonding out-of-plane trimetal a_2'' HOMO model[13] (under D_{3h} symmetry). These conclusions are also consistent with extended Hückel calculations recently reported by Schilling and Hoffmann[14] on a variety of $M_3(CO)_9(L)$ and $M_3(\eta^5\text{-}C_5H_5)_3(L)$ complexes (where M = Fe, Co, L = ligand) including the unknown $Co_3(\eta^5\text{-}C_5H_5)_3(\mu_3\text{-}CO)_2$, a 46-electron system of assumed D_{3h} symmetry. An extrapolation to $Ni_3(\eta^5\text{-}C_5H_5)_3(\mu_3\text{-}CO)_2$ by the addition of three electrons to their general energy-level scheme results in the unpaired electron occupying the a_2' HOMO.

The fact that electrochemical measurements[10] of these two neutral $CoNi_2$ molecules showed that they could be readily reduced to the corresponding monoanions provided a further incentive to "cement" our conclusions by determining the geometrical influence due to the addition of the unpaired electron to give an electronically equivalent analogue of the Fischer–Palm trinickel molecule. In addition, since cyclic voltammograms of the trinickel molecule indicated a chemically reversible one-electron reduction[15] (but not oxidation), we deemed it worthwhile to try to isolate its monoanion in that magnetic susceptibility measurements would then hopefully ascertain the presumed nondegeneracy of the proposed HOMO while X-ray diffraction measurements of the monoanion would provide a further detailed appraisal of the geometrical change upon adding a second "antibonding" electron. At the same time, we became interested in finding out whether the corresponding (pentamethylcyclopentadienyl)nickel carbonyl analogue of the Fischer–Palm molecule could be prepared. It was our prejudice that the composite effects of electronic change (due to the more electron-releasing C_5Me_5 rings relative to the C_5H_5 rings) and marked steric difference (due to the bulky methyl substituents) would change the energetics (but not the relative energy ordering) of the frontier MO's of the trinickel cluster to such an extent that a comparative examination of its redox properties would provide insight concerning the inherent stability of the Fischer–Palm molecule with respect to oxidation.

Herein are presented the results of our studies, which in our minds have fulfilled all of the above expectations in providing a much better understanding of the stereochemistry and bonding of the classical Fischer–Palm molecule and related triangular metal clusters.

Experimental Section

Preparation and Properties. The following experimental work was done under rigorous exclusion of air and water via Schlenk-type apparatus with dry N_2 (<3 ppm of O_2) as the inert atmosphere. Tetrahydrofuran was distilled from benzophenone ketyl and hydrocarbon solvents were distilled from CaH_2. Naphthalene and acenaphthalene were sublimed before use. $Ni_3(\eta^5\text{-}C_5H_5)_3(\mu_3\text{-}CO)_2$ was prepared by the method of Fischer and Palm,[8] while $(\eta^5\text{-}C_5Me_5)CoNi_2(\eta^5\text{-}C_5H_5)_2(\mu_3\text{-}CO)_2$ was synthesized by the method of Byers, Uchtman, and Dahl.[10]

(a) $[K(2,2,2\text{-crypt})]^+[(\eta^5\text{-}C_5Me_5)CoNi_2(\eta^5\text{-}C_5H_5)_2(\mu_3\text{-}CO)_2]^-\cdot 0.5(n\text{-}C_5H_{12})$. The corresponding neutral cobaltdinickel cluster (1 mmol, 0.497 g) and 1 mmol (0.376 g) of 2,2,2-crypt, $N(C_2H_4OC_2H_4OC_2H_4)_3N$ (PCR Research Chemicals, Inc.), were dissolved in 50 mL of THF. To this solution was added 1.1 equiv of potassium naphthalenide in THF. The mixture was allowed to stir for 30 min, after which 150 mL of pentane was added. The resulting precipitate was washed 3 times with 100 mL of pentane and then twice with 50 mL of a 1/1 mixture (v/v) of pentane/toluene. The resulting yield of $[K(2,2,2\text{-crypt})]^+[(\eta^5\text{-}C_5Me_5)CoNi_2(\eta^5\text{-}C_5H_5)_2(\mu_3\text{-}CO)_2]^-\cdot 0.5(n\text{-pentane})$ is nearly quantitative. The presence in the isolated crystalline sample of 0.5 *n*-pentane solvent molecule per formula unit was determined via the resulting X-ray crystallographic analysis (vide infra). An infrared spectrum (Beckman 4240 spectrophotometer) in THF solution showed one triply bridging carbonyl absorption band at 1680 cm^{-1}. This air-sensitive solid compound, which is especially unstable in solution, in soluble in CH_2Cl_2, THF, and acetonitrile (which must be rigorously dried and O_2 free). Room-temperature magnetic susceptibility measurements determined by the Faraday method at five different field strengths of range 5.9–7.9 kG gave relatively constant molar susceptibility values. The mean value of $\chi_g = 8.8 \times 10^{-4}$ cgs units (corrected for the diamagnetism of the ligands) corresponds to a magnetic moment of 1.45 μ_B which is in accordance with that expected for one unpaired electron in the monoanion. Its somewhat low value relative to the spin magnetic-moment value of 1.73 μ_B for one unpaired electron may be attributed (at least in part) to the air-sensitive sample being somewhat oxidized to the neutral diamagnetic parent. Electron paramagnetic resonance spectra of a concentrated THF solution of the compound in a sealed quartz tube were obtained at 77 K with a Varian E-15 spectrometer operating at 9.061 GHz. A typical spectrum exhibited an eight-line cobalt hyperfine pattern (characteristic of the interaction of the unpaired electron with the ^{59}Co nucleus (100% abundance, $I = {}^7/_2$)) centered about $g = 2.01$ with a hyperfine splitting constant of 27 G.

(b) $[K(2,2,2\text{-crypt})]^+[Ni_3(\eta^5\text{-}C_5H_5)_3(\mu_3\text{-}CO)_2]^-$. The synthesis and isolation of this salt were analogous to the above procedure except that a milder reducing agent, potassium acenaphthalenide, was used in that the use of potassium naphthalenide was found to produce an apparent decomposition during the reaction. An infrared spectrum of a THF solution of this red monoanion (**4**) of the Fischer–Palm neutral parent (**3**) gave a triply bridging carbonyl absorption band at 1712 cm^{-1}. This compound likewise is air sensitive, especially in solution. It readily dissolves in CH_2Cl_2, THF, and CH_3CN to give intensely red solutions.

(c) $Na^+[Ni_3(\eta^5\text{-}C_5H_5)_3(\mu_3\text{-}CO)_2]^-\cdot n$THF. This air-sensitive salt was prepared in nearly quantitative yield by the one-electron reduction of the corresponding trinickel cluster with an equimolar amount of $NaBH_4$ in THF solution at room temperature for 18 h. An infrared spectrum of this salt, which is sparingly soluble in THF and acetonitrile, revealed three triply bridging bands at 1712 (m), 1675 (m), and 1631 (s) cm^{-1}. The multiplet of the carbonyl bands is readily attributed to the occurrence of Na^+–O(carbonyl) ion pairing in THF solution. A solid-state infrared spectrum (Nujol mull) gave one broad carbonyl absorption peak at 1710 cm^{-1}. Magnetic susceptibility measurements via the Faraday method conclusively showed this salt to be diamagnetic ($\chi_g = 0.15 \times 10^{-6}$ cgs units, 20 °C).

(d) $Li^+[Ni(\eta^5\text{-}C_5Me_5)(CO)]^-\cdot n$THF. Attempts to synthesize $Ni_2(\eta^5\text{-}C_5Me_5)_2(\mu_2\text{-}CO)_2$ by the literature method[16] (without oxidation) were

(7) Nelson, L. L.; Lo, F. Y.-K.; Rae, A. D.; Dahl, L. F. *J. Organomet. Chem.* **1982**, *225*, 309–329.
(8) Fischer, E. O.; Palm, C. *Chem. Ber.* **1958**, *91*, 1725–1731.
(9) (a) Vahrenkamp, H.; Uchtman, V. A.; Dahl, L. F. *J. Am. Chem. Soc.* **1968**, *90*, 3272–3273. (b) Frisch, P. D.; Dahl, L. F. *Ibid.* **1972**, *94*, 5082–5084. (c) Uchtman, V. A.; Dahl, L. F. *Ibid.* **1969**, *91*, 3763–3769.
(10) Byers, L. R.; Uchtman, V. A.; Dahl, L. F. *J. Am. Chem. Soc.* **1981**, *103*, 1942–1951.
(11) Both $Ni_3(\eta^5\text{-}C_5H_5)_3(\mu_3\text{-}CO)_2$ and $CoNi_2(\eta^5\text{-}C_5H_5)_3(\mu_3\text{-}CO)_2$ crystallize with two molecules in a hexagonal unit cell of $P6_3/m$ symmetry, which thereby imposes crystallographic C_{3h}—$3/m$ site symmetry on each molecule. This results in the $CoNi_2$ molecule, which is presumably distorted in an analogous fashion to that determined for the crystal-ordered $(\eta^5\text{-}C_5Me_5)CoNi_2(\eta^5\text{-}C_5H_5)_2(\mu_3\text{-}CO)_2$ molecule, possessing an average disordered structure of threefold rotational symmetry in the crystalline state.
(12) (a) Strouse, C. E.; Dahl, L. F. *Discuss. Faraday Soc.* **1969**, *47*, 93–106. (b) Strouse, C. E.; Dahl, L. F. *J. Am. Chem. Soc.* **1971**, *93* 6032–6041.
(13) Longuet-Higgins, H. C.; Stone, A. *J. Mol. Phys.* **1962**, *5*, 417–424.
(14) Schilling, B. E. R.; Hoffmann, R. *J. Am. Chem. Soc.* **1979**, *101*, 3456–3467.
(15) Dessy, R. E.; Weissman, P. M.; Pohl, R. L. *J. Am. Chem. Soc.* **1966**, *88*, 5117–5121.
(16) Mise, T.; Yamazaki, H. *J. Organomet. Chem.* **1979**, *164*, 391–400.

unsuccessful; the solution product[17-20] obtained by us from the reported reaction of lithium pentamethylcyclopentadienide with nickel tetracarbonyl in THF under nonoxidizing conditions is most likely the orange-black monomeric $[Ni(\eta^5\text{-}C_5Me_5)(CO)]^-$ anion as the lithium salt. This formulation is completely consistent with its observed IR spectrum in THF solution exhibiting one strong carbonyl frequency at 1975 cm^{-1}, which is in the expected terminal carbonyl range for a monoanion.[21] Oxidation of this monoanion gives rise to the neutral nickel dimer.

(e) $Ni_2(\eta^5\text{-}C_5Me_5)_2(\mu_2\text{-}CO)_2$. This desired dimeric precursor was obtained in good yield from the oxidation of a THF solution of the generated Li^+ $[Ni(\eta^5\text{-}C_5Me_5)(CO)]^-$ with CuCl. In a typical experiment, pentamethylcyclopentadiene (25 mmol; 4.2 mL) was dissolved in 200 mL of THF and then deprotonated by addition of *n*-BuLi (19 mL of 1.6 M solution in hexane as obtained from Aldrich). To the resulting suspension of $Li(C_5Me_5)$ was added 5 mL (37 mmol) of $Ni(CO)_4$ dissolved in 20 mL of THF. A refluxing of this mixture for 8 h gave $Li^+[Ni(\eta^5\text{-}C_5Me_5)(CO)]^-$ in THF solution. To this solution product was added 25 mmol (2.47 g) of CuCl, after which the mixture was refluxed for an additional 2 h. During this time, the solution changed color from orange-black to red. Removal in vacuo of the solvent, $Ni(CO)_4$, and excess pentamethylcyclopentadiene gave a solid residue, from which the $Ni_2(\eta^5\text{-}C_5Me_5)_2(\mu_2\text{-}CO)_2$ dimer was extracted with several 50-Ml portions of pentane. Evaporation of the solvent gave the crystalline dimer in sufficiently pure form for subsequent chemical reactions. Yields, which varied somewhat from preparation to preparation, usually ranged between 50 and 60% (2.7–3.2 g). High-purity dimer was obtained by chromatography of the product on a neutral, deactivated alumina column with pentane as an eluant, followed by sublimation at 90 °C (10^{-3} torr). The (pentamethylcyclopentadienyl)nickel carbonyl dimer is best stored at −20 °C under an inert atmosphere, as slow decomposition appears to occur at room temperature. Its infrared fingerprinting spectrum in cyclohexane solution of two maxima in the bridging carbonyl region at 1815 and 1858 cm^{-1} is in excellent agreement with that determined by Mise and Yamazaki,[16] who have examined its spectroscopic properties and reactivites relative to those of the corresponding unsubstituted cyclopentadienylnickel carbonyl dimer.

(f) $Ni_3(\eta^5\text{-}C_5Me_5)_3(\mu_3\text{-}CO)_2$. This sought-after compound was produced by the photochemical reaction of the above-prepared nickel dimer and nickelocene. In an illustrative experiment, 0.027 g (4.2 mmol) of $Ni_2(\eta^5\text{-}C_5Me_5)_2(\mu_2\text{-}CO)_2$ and 0.150 g (7.9 mmol) of nickelocene were dissolved in 50 mL of toluene, and the solution was photolyzed for 14 h with a Hanovia 450-W ultraviolet lamp in a quartz glass cell. The solution changed color from red to blackish yellow during the course of the reaction. Removal of the solvent by evaporation gave rise to a green crystalline solid, which was dissolved in a minimum amount of Skelly B and then loaded onto a column (2 cm in diameter; 20 cm in length) of neutral grade III alumina. Elution with hexane afforded a faint nickelocene band followed by a brown band. Subsequent removal of the solvent from this latter band yielded ca. 20 mg of a green crystalline solid identified as $Ni_3(\eta^5\text{-}C_5Me_5)_3(\mu_3\text{-}CO)_2$. Further elution with hexane/benzene produced faint brown-green bands which are presumed to correspond to analogous triangular nickel dicarbonyl clusters with mixed cyclopentadienyl and pentamethylcyclopentadienyl ligands. An infrared spectrum of $Ni_3(\eta^5\text{-}C_5Me_5)_3(\mu_3\text{-}CO)_2$ in cyclohexane solution exhibits a single carbonyl peak at 1700 cm^{-1}. This molecular compound is soluble in a variety of nonpolar organic solvents. A cyclic voltammetric study of this cluster was carried out with a PAR electrochemical system. The measured sample was a ca. 1×10^{-3} M solution of the trinickel cluster dissolved in THF with a 0.1 M concentration of TBAH as the supporting electrolyte. The reference electrode was a Ag/Ag^+ couple and the working electrode used was a gold disk. Preparation of the sample solution and the electrochemical experiment were carried out under a nitrogen atmosphere. The $E_{1/2}$ values (uncorrected for junction potentials but corrected for internal resistance potential drop) for the three determined couples[22] $[Ni_3]^0/[Ni_3]^-$, $[Ni_3]^+/[Ni_3]^0$, $[Ni_3]^{2+}/[Ni_3]^+$ (where Ni_3 denotes **5**) are −1.12, −0.35, and +0.08 V, respectively. The peak-to-peak separations for the three couples ($E_{p,c} - E_{p,a}$) are 245, 260, and 270 mV, respectively, for a scan rate of 500 mV/s. The ratio of the anodic and cathodic peak currents, $i_{p,a}$ and $i_{p,c}$, is near unity for each couple. Hence, the three couples may be described as chemically reversible.

X-ray Data Collections. Crystallographic structural determinations were performed for three compounds—viz., $[K(2,2,2\text{-crypt})]^+[(\eta^5\text{-}C_5Me_5)CoNi_2(\eta^5\text{-}C_5H_5)_2(\mu_3\text{-}CO)_2]^-\cdot 0.5(n\text{-}C_5H_{12})$ (**2**), $[K(2,2,2\text{-crypt})]^+[Ni_3(\eta^5\text{-}C_5H_5)_3(\mu_3\text{-}CO)_2]^-$ (**4**), and $Ni_3(\eta^5\text{-}C_5Me_5)_3(\mu_3\text{-}CO)_2$ (**5**). Suitable crystals of **2** and **4** were obtained by a slow solvent diffusion of pentane into a THF solution of the salt under N_2 atmosphere. Crystals of **5** were isolated from a slow evaporation of a cyclohexane solution. In each case a parallelepiped-shaped crystal (of approximate dimensions $0.50 \times 0.30 \times 0.20$ mm for **2**, $0.50 \times 0.30 \times 0.30$ mm for **4**, $0.35 \times 0.40 \times 0.10$ mm for **5**) was mounted inside a Lindemann glass capillary which was evacuated, filled with argon, and then hermetically sealed. A Syntex (Nicolet) $P\bar{1}$ diffractometer with Mo $K\alpha$ radiation was used to obtain intensity data at room temperature (ca. 22 °C) by the θ–2θ scan technique. Details of the crystal alignment and data-collection parameters along with a listing of the utilized crystallographic programs (in addition to the ones specifically mentioned herein) are given elsewhere.[23] For **2**, intensities were sampled once for four independent reciprocal-lattice octants (corresponding to a chosen body-centered triclinic unit cell) over the range $3.0° < 2\theta < 45.0°$; data reduction gave 6136 independent reflections with 3242 possessing $I > 2\sigma(I)$. For **4**, intensities were measured once over the range $3.0° < 2\theta < 45.0°$ for two independent monoclinic octants; data reduction yielded 5073 independent data with 2141 having $I > 2\sigma(I)$. For **5**, whose Laue symmetry conforms to hexagonal D_{6h}—$6/m2/m2/m$, data reduction of the intensities collected for the *hkl* octant over the range $3.0° < 2\theta < 60.0°$ gave 974 independent data with 656 possessing $I > 2\sigma(I)$.

A correction of the intensity data of **2** for a crystal decay was made on the basis of two standard reflections (monitored after every 48 data), each exhibiting an analogous linear-like decrease of ca. 11% during the data collection. For both **4** and **5**, the standard reflections showed no intensity variations greater than 3% during the entire data collection. Empirical absorption corrections (based on Ψ scans) of the intensities were made for all three compounds.

Unit Cell Data. (a) $[K(2,2,2\text{-crypt})]^+[(\eta^5\text{-}C_5Me_5)CoNi_2(\eta^5\text{-}C_5H_5)_2(\mu_3\text{-}CO)_2]^-\cdot 0.5(n\text{-}C_5H_{12})$. The determined lattice constants obtained for the triclinic unit cell are $a = 14.988$ (5) Å, $b = 24.507$ (10) Å, $c = 12.988$ (6) Å, $\alpha = 84.52$ (4)°, $\beta = 92.70$ (1)°, and $\gamma = 80.09$ (3)°. The unit cell volume of 4668 (3) Å^3 and $M_r = 946.47$ for $CoNi_2KO_8N_2C_{42.5}H_{67}$ give rise to a calculated density of 1.35 g/cm^3 for $Z = 4$. The total number of electrons in the unit cell, $F(000)$, is 2008.

Observed systematic absences of $\{hkl\}$ for $h + k + l = 2n + 1$ indicate a body-centered unit cell consistent with the probable space groups being either $I1$ or $I\bar{1}$; our choice of the latter centrosymmetric space group, which is a nonstandard space group of $P\bar{1}(C_i^1$, No. 2), was confirmed by the successful solution of the crystal structure. For a reduced triclinic unit cell of $P\bar{1}$ symmetry with $Z = 2$, the lattice constants are $a = 14.039$ Å, $b = 14.988$ Å, $c = 12.988$ Å, $\alpha = 92.70°$, $\beta = 110.74°$, $\gamma = 111.21°$, and $V = 2334$ Å^3.

(17) Although this compound was not isolated and characterized in the solid state, the well-known great affinity of the lithium ion for THF molecules in the formation of tight Li^+–O(THF) ion pairing[18-20] makes it extremely likely that the crystalline compound has *n* THF solvent molecules.

(18) Ginsburg, R. E.; Berg, L. M.; Rothrock, R. K.; Collman, J. P.; Hodgson, K. O.; Dahl, L. F. *J. Am. Chem. Soc.* **1979**, *101*, 7218–7231 and references cited therein.

(19) Darensbourg, M. Y.; Burns, D. *Inorg. Chem.* **1974**, *13*, 2970–2973.

(20) Darensbourg, M. Y.; Darensbourg, D. J.; Burns, D.; Drew, D. A. *J. Am. Chem. Soc.* **1976**, *98*, 3127–3136 and references cited therein.

(21) The absence of carbonyl multiplet peaks due to contact Li^+–O (carbonyl) interactions in THF solution may be readily attributed to their relative strength being considerably less than that for Li^+–O(THF) interactions. This preference for Li^+–solvent ion pairs is in harmony with the findings in the solution state by the Darensbourgs and co-workers[19,20] who carried out a comprehensive study via infrared, kinetic, and conductivity measurements of solvent effects on alkali metal interactions with *trans*-phenylacyltricarbonyl(triphenylphosphine)iron(−1) monoanion[19] and with several different phosphine derivatives of the maganese carbonylate monoanion.[20] For these species they observed that a complete breakdown of contact Li^+–O(carbonyl) ion pairing occurred in THF, in contrast to the existence of contact Na^+–O(carbonyl) ion pairing in THF. They ascribed their findings as being consistent with the expected increased stability of a $Li^+\cdot n$THF solvate over a $Na^+\cdot n$THF solvate.[20] It is noteworthy that these results are also completely compatible with our observations of a plethora of carbonyl frequencies (rather than the expected one with no ion pairing) in the infrared spectrum of the Na^+ salt of the $[Ni_3(\eta^5\text{-}C_5H_5)_3(\mu_3\text{-}CO)_2]^-$ monoanion in THF solution vs. the expected one-carbonyl frequency in the infrared spectrum of the lithium salt of the $[Ni(\eta^5\text{-}C_5Me_5)(CO)]^-$ monoanion in THF solution.

(22) The particular assignment of the three couples was done by an electrolysis experiment which measured current vs. voltage for a rapidly agitated solution. The purpose of this "minielectrolysis" experiment is to determine the voltage range through which no current flows—i.e., the voltage range through which the bulk solution species (in the present case the *neutral* trinickel cluster) is electrochemically stable. As one sweeps past the zero-current range to more positive voltage, any current that flows must be due to oxidation processes (i.e., any electrochemical couples occurring in the range correspond to oxidations). Upon a negative sweeping of the zero-current region, any current flow will show the presence of reduction processes, which allows for an assignment of couples occurring in this region. It is noteworthy that this procedure is not an exhaustive electrolysis and thus does not give unambiguous information concerning the number of electrons involved in each oxidation or reduction process.

(23) Byers, L. R.; Dahl, L. F. *Inorg. Chem.* **1980**, *19*, 277–284.

(b) $[K(2,2,2\text{-crypt})]^+[Ni_3(\eta^5\text{-}C_5H_5)_3(\mu_3\text{-}CO)_2]^-$. The lattice constants obtained for the monoclinic unit cell are a = 10.203 (3) Å, b = 17.630 (8) Å, c = 21.730 (9) Å, and β = 98.00 (3)°. On the basis of the unit cell volume of 3871 (3) Å^3 and M_r = 843.03 for $Ni_3KO_8N_2Co_{35}H_{51}$, the calculated density is 1.48 g/cm^3 for Z = 4, and $F(000)$ = 1824.

Systematic absences $\{h0l\}$ for $h + l = 2n + 1$ and $\{0k0\}$ for $k = 2n + 1$ uniquely point to the probable space group being $P2_1/n$ (nonstandard setting of $P2_1/c$ (C_{2h}^5, No. 14)).

(c) $Ni_3(\eta^5\text{-}C_5Me_5)_3(\mu_3\text{-}CO)_2$. The lattice constants for the determined hexagonal unit cell are $a = b$ = 10.761 (4) Å, c = 15.348 (3) Å, and V = 1538 (1) Å^3. The observed density (measured by the flotation method) of 1.36 g/cm^3 agrees within experimental error (±0.02 g/cm^3) with the calculated value of 1.38 g/cm^3 for Z = 2 and a M_r = 637.84 for $Ni_3O_2C_{32}H_{45}$. $F(000)$ is 674.

Observed systematic absences of $\{00l\}$ for $l = 2n + 1$ uniquely conform to $P6_322$ (D_{6h}^6, No. 182) as the probable space group under D_{6h} Laue symmetry. This space group is the same as that previously found for $Ni_3(\eta^5\text{-}C_5H_5)_3(\mu_3\text{-}S)_2$[9a] and $Co_3(\eta^5\text{-}C_5H_5)_3(\mu_3\text{-}S)_2$,[9b] for which the crystal structures were solved by application of an incoherent twinning mechanism involving a single-crystal component of the above unit-cell dimensions and of $P6_3/m$ symmetry (vide infra).

Structural Determinations and Refinements

(a) $[K(2,2,2\text{-crypt})]^+[(\eta^5\text{-}C_5Me_5)CoNi_2(\eta^5\text{-}C_5H_5)_2(\mu_3\text{-}CO)_2]^-\cdot 0.5(n\text{-}C_5H_{12})$. The structural determination (whose resulting atomic parameters are based on the nonprimitive unit cell of $I\bar{1}$ symmetry) necessitated the locations of one monocation and one monoanion corresponding to 2 nickel, 1 cobalt, 1 potassium, 8 oxygen, 2 nitrogen, 40 carbon, and 61 hydrogen atoms, each occupying the fourfold set of general positions (0, 0, 0; $^1/_2$, $^1/_2$, $^1/_2$) ± (x, y, z).

The crystal structure of **2** was solved from direct-method analysis by application of MULTAN[24] followed by successive Fourier syntheses, which revealed the locations of all nonhydrogen atoms in both the monocation and monoanion. In addition, five independent peaks of similar electron density (which on a difference Fourier map corresponded to the five highest residual density maxima) were discovered about a center of inversion. Their arrangement in an open zig-zag configuration with a separation of ca. 1.4 Å between adjacent peaks resulted in their assignment to a disordered pentane molecule randomly occupying either one site or its centrosymmetrically related site (i.e., the occupation by two whole-weighted pentane molecules of both sites about a center of symmetry in a given unit cell can be readily excluded from the resulting intermolecular C···C separations being too close to one another). At this point idealized coordinates were calculated[25] for the hydrogen atoms of the cryptate ligand and C_5H_5 rings (but not of the C_5Me_5 ring and pentane molecule of crystallization). These idealized positions for the hydrogen atoms were not varied during the least-squares refinement but were recalculated after every other cycle so as to take into account the shifts in positions of the attached carbon atoms. The hydrogen thermal parameters were constrained to a fixed isotropic value. Anisotropic least-squares refinement of all nonhydrogen atoms with the program RAELS[25] reduced the discrepancy indices to $R_1(F)$ = 9.1% and $R_2(F^2)$ = 8.8%[26-28] for the 3242 observed reflections. The goodness-of-fit parameter[26] was 1.48. A final Fourier difference map revealed no anomalous features. The atomic parameters from the output of the last least-squares cycle are available as supplementary material along with the observed and calculated structure factor amplitudes. Interatomic distances and bond angles are presented in Table I.

(b) $[K(2,2,2\text{-crypt})]^+[Ni_3(\eta^5\text{-}C_5H_5)_3(\mu_3\text{-}CO)_2]^-$. The crystallographically independent unit consists of one entire formula unit corresponding to 3 nickel, 1 potassium, 8 oxygen, 2 nitrogen, 35 carbon, and 51 hydrogen atoms each occupying under $P2_1/n$ symmetry the fourfold set of general positions ±(x, y, z; $^1/_2 + x$, $^1/_2 - y$, $^1/_2 + z$).

The crystal structure was elucidated from the use of MULTAN[24] followed by successive Fourier syntheses which located all the nonhydrogen atoms. Least-squares refinement was then carried out with RAELS[25] under the following boundary conditions: (1) The potassium, nickel, and carbonyl atoms are refined with individual anisotropic thermal parameters. (2) Each C_5H_5 ring, whose coordinates were idealized to a regular pentagon of D_{5h} symmetry with fixed C–C and C–H bond lengths of 1.40 and 0.95 Å, respectively, was refined as a rigid body (involving 6 variable parameters) with its thermal motion[29] described by a TLX model (involving 15 variables).[30] (3) All nonhydrogen atoms of the cryptate ligand were refined with individual positions and anisotropic thermal parameters, but weighted geometrical (or slack) constraints[31] were imposed; these included a minimization of the bond-length differences (ideally zero) among the set of C–C bonds, among the set of C–N bonds, and among the set of C–O bonds such that the individual members of each set refined toward the same value which is a priori unspecified. The tetrahedral-like bond angles of the cryptate ligand were more loosely constrained about an idealized value of 109.5°. Coordinates for the methylene hydrogen atoms were miraged[25] at idealized tetrahedral-like positions at 0.95 Å from their respective carbon atoms. These hydrogen atoms (with each given a constant isotropic temperature factor) were included as fixed-atom contributors in the least-squares refinement, but their idealized positions were recalculated after every other cycle. The resulting refinement converged at $R_1(F)$ = 8.4% and $R_2(F^2)$ = 10.8%[26-28] for the 2141 observed data; the goodness-of-fit parameter[26] was 1.49. A final Fourier difference map showed no unusual features. The atomic parameters from the output of the least-squares cycle, together with the observed and calculated structure factor amplitudes, are given as supplementary material. Table II presents appropriate interatomic distances and bond angles.

(c) $Ni_3(\eta^5\text{-}C_5Me_5)_3(\mu_3\text{-}CO)_2$. On the basis of the crystal data of **5** being similar to that previously encountered for $Ni_3(\eta^5\text{-}C_5H_5)_3(\mu_3\text{-}S)_2$[9a] and $Co_3(\eta^5\text{-}C_5H_5)_3(\mu_3\text{-}S)_2$,[9b] an analogous incoherent twinning model involving an individual hexagonal single-crystal component of symmetry $P6_3/m$ was used to solve its crystal structure. Details of the procedure for unraveling the observed $|F_o|^2$ data for the twin composite into the appropriate $|F_o|$ coefficients for the single-crystal component were developed by Wei[32] for solving and refining such twinned structures and are given elsewhere.[9] The single-crystal component $|F_o|$ data were utilized to determine the positions of the independent nickel atom from a Patterson analysis. The space group $P6_3/m$ requires each of the two equivalent molecules of **5** per cell to possess crystallographic C_{3h}—$3/m$ site symmetry with the two mirror-related carbonyl ligands lying on the threefold axis and with each of its threefold-related C_5Me_5 rings either in an ordered orientation bisected by the horizontal mirror plane or in two mirror-related disordered orientations. Least-squares refinement was performed with RAELS[25] in which individual positional and anisotropic thermal parameters were varied for each nonhydrogen atom. Weighted geometric constraints,[31] in which the C(ring)–C(ring) and C(ring)–C(methyl) distances were held at 1.40 and 1.54 Å, respectively, were used to aid the refinement of the pentamethylcyclopentadienyl rings. Both ordered and disordered models (which omitted the methyl hydrogen atoms) were used to refine the C_5Me_5 ring, with the best model involving an ordered ring bisected by the horizontal mirror plane at $z = {}^3/_4$. This refinement converged at $R_1(F)$ = 9.1% and $R_2(F^2)$ = 12.2%[26-28] for the 656 observed data; the goodness-of-fit value[26] was 2.02. A final Fourier difference map exhibited no unusual features. The resulting atomic parameters from the last cycle are available as supplementary material together with the observed and calculated structure factor amplitudes. Appropriate distances and bond angles are presented in Table III.

Results and Discussion

Structural Features of $[K(2,2,2\text{-crypt})]^+(\eta^5\text{-}C_5Me_5)CoNi_2(\eta^5\text{-}C_5H_5)_2(\mu_3\text{-}CO)_2]^-\cdot 0.5(n\text{-}C_5H_{12})$. There is no evidence from interionic contacts of any specific ion-pair interactions, in contrast to those established[6b,33] in $[K(2,2,2\text{-crypt}]^+$ salts of other metal

(24) Main, P.; Lessinger, L.; Woolfson, M. M.; Germain, G.; Declercq, J.-P. "MULTAN-76", an updated version of MULTAN: Germain, G.; Main, P.; Woolfson, M. M. *Acta Crystallogr., Sect. A* **1971**, *A27*, 368–376.

(25) Rae, A. D. "RAELS, A Comprehensive Least-Square Program"; University of New South Wales, Kensington, 1976. Adapted for a Harris/7 computer by A. D. Rae, University of Wisconsin—Madison, 1980.

(26) The unweighted and weighted discrepancy factors used are $R_1(F) = [\sum||F_o| - |F_c||/\sum|F_o|] \times 100$ and $R_2(F^2) = [\sum w_i||F_o|^2 - |F_c|^2|^2/\sum w_i|F_o|^4]^{1/2} \times 100$. All least-squares refinements were based on the minimization of $\sum w_i||F_o|^2 - |F_c|^2|^2$ with individual weights of $w_i = 1/\sigma(F_o)$ assigned on the basis of the esd's of the observed structure factors. The standard deviation in an observation of unit weight ("goodness-of-fit") is defined by $[\sum w_i(|F_o| - ||F_c|)^2/(m - n)]^{1/2}$, where m is the number of independent number of data and n the number of parameters varied in the refinement.

(27) The scattering factor tables used are those of Cromer and Mann[28a] for the nonhydrogen atoms and those of Stewart et al.[28b] for the hydrogen atoms. Real and imaginary corrections for anomalous dispersion[28c] were included in the structure factor calculations.

(28) (a) Cromer, D. T.; Mann, J. B. *Acta Crystallogr., Sect. A* **1968**, *A24*, 321–324. (b) Stewart, R. F.; Davidson, E. R.; Simpson, W. T. *J. Chem. Phys.* **1965**, *42*, 3175–3187. (c) "International Tables for X-Ray Crystallography"; Kynoch Press: Birmingham, England, 1974; Vol. IV, p 149.

(29) Schomaker, V.; Trueblood, K. N. *Acta Crystallogr., Sect. B* **1968**, *B24*, 63–76.

(30) Rae, A. D. *Acta Crystallogr., Sect. A* **1975**, *A31*, 570–574.

(31) (a) Waser, J. *Acta Crystallogr.* **1963**, *16*, 1091–1094. (b) Rae, A. D. *Ibid. Sect. A* **1978**, *A34*, 578–582.

(32) (a) Wei, C. H. "Abstracts of Papers", National Meeting of the American Crystallographic Association, University of Minnesota, Minneapolis, MN, August 20–25, 1967; p 83. (b) Wei, C. H.; Wilkes, G. R.; Dahl, L. F. *J. Am. Chem. Soc.* **1967**, *89*, 4792–4793. (c) Wei, C. H. *Inorg. Chem.* **1969**, *8*, 2384–2397.

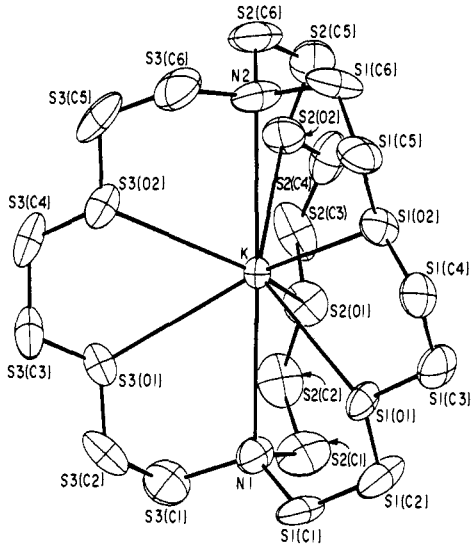

Figure 1. $[K(2,2,2\text{-crypt})]^+$ monocation of the $[(\eta^5\text{-}C_5Me_5)CoNi_2(\eta^5\text{-}C_5H_5)_2(\mu_3\text{-}CO)_2]^-$ salt.

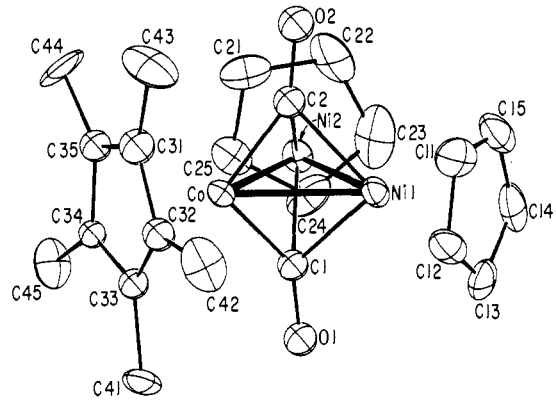

Figure 2. $[(\eta^5\text{-}C_5Me_5)CoNi_2(\eta^5\text{-}C_5H_5)_2(\mu_3\text{-}CO)_2]^-$ monoanion (of crystallographic C_1–1 site symmetry) crystallized as the $[K(2,2,2\text{-crypt})]^+$ salt.

cluster anions. A *n*-pentane molecule of crystallization was found about one inversion center in the unit cell to be randomly distributed in two centrosymmetrically related orientations.

The configuration (Figure 1) of the $[K(2,2,2\text{-crypt})]^+$ cation appears to be reasonably normal with the K^+ ion symmetrically imbedded in the cavity of two nitrogen and six oxygen atoms. The six cryptand oxygen atoms nearly conform to a trigonal prism as indicated by an average twist angle α of ca. 7° (where $\alpha = 0°$ when the two oxygen triangles form an eclipsed conformation about the pseudo-threefold rotation axis).

An examination of Figure 2 shows that the overall configuration of the $[(\eta^5\text{-}C_5Me_5)CoNi_2(\eta^5\text{-}C_5H_5)_2(\mu_3\text{-}CO)_2]^-$ monoanion, **2**, is analogous to that of its neutral precursor, **1**, with two triply bridging carbonyl ligands capping the triangularly coordinated metal atoms of one $Co(\eta^5\text{-}C_5Me_5)$ and two $Ni(\eta^5\text{-}C_5H_5)$ fragments. The geometry of its $CoNi_2(CO)_2$ core depicted in Figure 3 experimentally conforms to C_{2v}—$mm2$ symmetry. The nearly symmetrical coordination in **2** of the pentamethylcyclopentadienyl ligand to the cobalt atom and of each cyclopentadienyl ligand to its nickel atom is evidenced by the 2.079 (12)–2.118 (12) Å range for the five Co–C(ring) bond lengths and by the 2.153 (14)–2.196 (14) Å range for the 10 Ni–C(ring) bond lengths. An analogous symmetrical linkage of these ligands to their respective metal atoms was also observed[10] in **1**.

Comparison between the Geometries of $[(\eta^5\text{-}C_5Me_5)CoNi_2(\eta^5\text{-}C_5H_5)_2(\mu_3\text{-}CO)_2]^n$ (n = 0, 1–) and Resulting Bonding Implications. The one-electron reduction of the parent **1** to its monoanion **2** preserves the approximate C_{2v} geometry of the $CoNi_2(CO)_2$ core but produces pronounced bond-length alterations within it together with small but definite changes in the M–C(ring) bond lengths. An analysis of the mean molecular parameters of **1** and **2** (Table IV) reveals the following significant differences, which may be readily interpreted from electronic considerations.

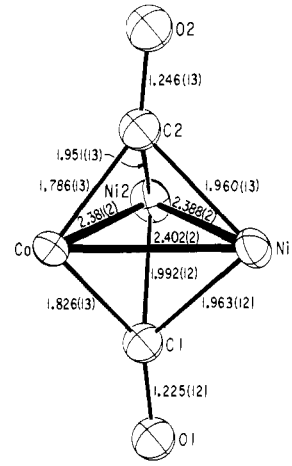

Figure 3. The $CoNi_2(CO)_2$ core of the $[(\eta^5\text{-}C_5Me_5)CoNi_2(\eta^5\text{-}C_5H_5)_2(\mu_3\text{-}CO)_2]^-$ monoanion, which contains one antibonding trimetal electron, experimentally conforms to C_{2v}—$2mm$ symmetry.

(a) Metal–Metal Distances. The most notable difference upon the formation of **2** from **1** is that the Ni–Ni bond in the monoanion has considerably enlarged by 0.062 Å from 2.326 (2) Å in **1** to 2.388 (2) Å in **2** relative to the smaller but still significant average increase in each of the two chemically equivalent Co–Ni bonds by 0.021 Å from 2.371 Å in **1** to 2.392 Å in **2**. These bond-length increases reflect the addition of the unpaired electron in **2** to an antibonding trimetal MO which for the $CoNi_2$ system has significantly greater nickel 3d AO character. The resulting mean value of 2.390 Å for the virtually identical Co–Ni and Ni–Ni bond lengths in **2** is experimentally the same as the value of 2.389 (2) Å found for the three crystallographically identical Ni–Ni distances in the redetermined structure[10] of the electronically equivalent Fischer–Palm $Ni_3(\eta^5\text{-}C_5H_5)_3(\mu_3\text{-}CO)_2$ molecule.

(b) Metal–Carbonyl Distances. Another striking observation is that both the Co–CO and Ni–CO bond lengths of the coordinately equivalent carbonyl ligands (under assumed C_{2v} symmetry) are considerably shorter in **2** than in **1**. The average Co–CO bond length for the two Co–CO bonds of 1.858 Å in **1** is reduced by 0.052 Å to 1.806 Å in **2**, while the average Ni–CO bond length of 2.014 Å for the four Ni–CO bonds in **1** is shortened by 0.047 Å to 1.967 Å in **2**. This opposite bond-length trend from the changes in the metal–metal distances as well as the similarly large asymmetry between the Co–CO and Ni–CO distances in both **1** and **2** may be readily attributed to strengthened d_π(metal) → π^*(CO) back-bonding in **2** relative to that in **1** due to the negative charge of the added electron raising up the trimetal energy levels to more closely match the corresponding π^*(CO) energy levels. The fact that the two Co–CO bond lengths are 0.15–0.16 Å shorter than the four Ni–CO bond lengths in both **1** and **2** has been ascribed[10] to the corresponding nickel 3d orbital energy levels being stabilized below the cobalt ones (and hence being further away from the π^*(CO) levels, on account of each nickel nucleus containing one more proton than the cobalt nucleus. The greater carbonyl interaction with the cobalt atom relative to that with each nickel atom gives rise to the Co–C–O bond angles being 15° larger than the Ni–C–O bond angles (viz. of 145° (av) vs. 130° in **1** and of 143° (av) vs. 128° (av) in **2**). The extent that the greater $d_\pi(M) \rightarrow \pi^*(CO)$ back-bonding in **2** relative to that in **1** produces a concomitant weakening of its C–O bonds (through increased electron density in the π^*(CO) orbitals) is indicated by the observed decrease (in THF solution) of 45 cm^{-1} in the carbonyl stretching frequency from 1725 cm^{-1} in **1** to 1680 cm^{-1} in **2**.

(33) Petersen, J. L.; Brown, R. K.; Williams, J. M. *Inorg. Chem.* **1981**, *20*, 158–165.

Table I. Interatomic Distances and Bond Angles for $[K(2,2,2\text{-crypt})]^+[(\eta^5\text{-}C_5Me_5)CoNi_2(\eta^5\text{-}C_5H_5)_2(\mu_3\text{-}CO)_2]^{-}\cdot{}^1/_2(n\text{-}C_5H_{12})$

A. Intraanion Distances[a] (Å)

Ni1–Ni2	2.388 (2)	Ni1–C11	2.164 (15)	Co–C31	2.092 (15)	C21–C22	1.370 (22)
		Ni1–C12	2.153 (14)	Co–C32	2.114 (13)	C22–C23	1.440 (27)
Co–Ni1	2.402 (2)	Ni1–C13	2.196 (14)	Co–C33	2.079 (12)	C23–C24	1.421 (25)
Co–Ni2	2.381 (2)	Ni1–C14	2.170 (16)	Co–C34	2.118 (12)	C24–C25	1.353 (20)
average	2.392	Ni1–C15	2.166 (15)	Co–C35	2.099 (13)	C25–C21	1.390 (18)
		average	2.170	average	2.100	average	1.395
Ni1–C1	1.963 (12)						
Ni2–C1	1.992 (12)	Ni2–C21	2.164 (13)	Ni1–Cp(1)[b]	1.813	C31–C32	1.439 (17)
Ni1–C2	1.960 (13)	Ni2–C22	2.156 (15)	Ni2–Cp(2)	1.813	C32–C33	1.360 (15)
Ni2–C2	1.951 (13)	Ni2–C23	2.159 (15)	Co–Cp(3)	1.721	C33–C34	1.402 (15)
average	1.967	Ni2–C24	2.169 (15)			C34–C35	1.441 (15)
		Ni2–C25	2.187 (13)	C11–C12	1.393 (19)	C35–C31	1.440 (17)
Co–C1	1.826 (13)	average	2.167	C12–C13	1.398 (21)	average	1.416
Co–C2	1.786 (13)			C13–C14	1.422 (20)		
average	1.806			C14–C15	1.420 (23)	C31–C41	1.548 (20)
				C15–C11	1.376 (22)	C32–C42	1.565 (19)
C1–O1	1.225 (12)			average	1.402	C33–C43	1.536 (17)
C2–O2	1.246 (13)					C34–C44	1.535 (17)
average	1.236					C35–C45	1.494 (18)
						average	1.536

B. Intraanion Bond Angles[a] (deg)

Ni2–Ni1–Co	59.62 (7)	Ni2–Ni1–C1	53.4 (4)	Ni1–C1–Co	78.6 (5)	C25–C21–C22	109 (2)
Ni1–Ni2–Co	60.47 (7)	Ni2–Ni1–C2	52.2 (4)	Ni2–C1–Co	77.0 (5)	C21–C22–C23	108 (2)
average	60.05	Ni1–Ni2–C1	52.3 (4)	Ni1–C2–Co	79.6 (5)	C22–C23–C24	105 (2)
		Ni1–Ni2–C2	52.5 (4)	Ni2–C2–Co	79.0 (5)	C23–C24–C25	109 (2)
Ni1–Co–Ni2	59.90 (7)	average	52.6 (4)	average	78.6	C24–C25–C21	109 (2)
						average	108
Ni1–Co–C1	53.2 (4)	C1–Ni1–C2	84.5 (5)	Ni1–C1–Ni2	74.3 (4)		
Ni2–Co–C1	54.6 (4)	C1–Ni2–C2	83.9 (5)	Ni1–C2–Ni2	75.3 (5)	C35–C31–C32	108 (1)
Ni1–Co–C2	53.4 (4)	average	84.2	average	74.8	C31–C32–C33	108 (1)
Ni2–Co–C2	53.6 (4)					C32–C33–C34	108 (1)
average	53.7	C1–Co–C2	93.8 (6)	C15–C11–C12	107 (2)	C33–C34–C35	108 (1)
				C11–C12–C13	111 (2)	C34–C35–C31	106 (1)
Co–Ni1–C1	48.2 (4)	Ni1–C1–O1	129.3 (9)	C12–C13–C14	105 (2)	average	108
Co–Ni1–C2	47.0 (4)	Ni2–C1–O1	128.0 (9)	C13–C14–C15	108 (2)		
Co–Ni2–C1	48.4 (4)	Ni1–C2–O2	127.6 (9)	C14–C15–C11	109 (2)	C35–C31–C41	124 (1)
Co–Ni2–C2	47.4 (4)	Ni2–C2–O2	128.3 (9)	average	108	C32–C31–C41	128 (1)
average	47.8	average	128.3			C31–C32–C42	124 (1)
						C33–C32–C42	128 (1)
		Co–C1–O1	143.7 (9)			C32–C33–C43	125 (1)
		Co–C2–O2	142.6 (9)			C34–C33–C43	124 (1)
		average	143.1			C33–C34–C44	128 (1)
						C35–C34–C44	123 (1)
						C34–C35–C45	126 (1)
						C31–C35–C45	128 (1)
						average	126

C. Intracation Distances (Å)

K···N1	3.019	K···S1(O1)	2.838	C–C	1.464 (av 9 dist)
K···N2	2.968	K···S1(O2)	2.784	C–N	1.465 (av 9 dist)
average	2.994	K···S2(O1)	2.752	C–O	1.404 (av 12 dist)
		K···S2(O2)	2.774	av tetrahedral angle = 111.6°	
		K···S3(O1)	2.829		
		K···S3(O2)	2.833		
		average	2.802		

[a] Values for the $CoNi_2(CO)_2$ core are averaged under assumed C_{2v} symmetry, while those involving each C_5R_5 ring are averaged under assumed C_{5v} symmetry. [b] Cp(*n*) denotes the centroid of the *n*th C_5R_5 ring.

(c) Metal–Cyclopentadienyl Distances. Table IV shows that the mean M–C(ring) bond lengths also signficantly enlarge on going from **1** to **2**. The mean of the 10 Ni–C(ring) bond lengths in **2** is 0.058 Å longer than that in **1**, while the mean of the five Co–C(ring) bond lengths in **2** is 0.026 Å longer than that in **1**. The sizably larger average increase in the Ni–C(ring) distances relative to the increase in Co–C(ring) distances appears to parallel the analogously larger increase in the Ni–Ni distance vs. the increase in the average Co–Ni distance. These particular trends may be rationaled in terms of the additional electron in **2** residing in an antibonding trimetal orbital with markedly greater nickel orbital character. It is apparent that the elongation by 0.036 Å in **1** and by 0.068 Å in **2** of the Ni–C(ring) bond lengths compared to the Co–C(ring) bond lengths is a consequence of the *net* stronger bonding of the more electron-releasing pentamethylcyclopentadienyl ligand to its attached cobalt atom than that of each unsubstituted cyclopentadienyl ligand to its coordinated nickel atom.

Structural Features of $[K(2,2,2\text{-crypt})]^+[Ni_3(\eta^5\text{-}C_5H_5)_3(\mu_3\text{-}CO)_2]^-$. In this salt the crystalline packing of the cations and anions, which are not constrained in special positions by crystallographic symmetry elements, is normal, with no unusual interionic contacts indicative of specific ion-pair interactions.

The $[K(2,2,2\text{-crypt})]^+$ monocation also exhibits no abnormal structural features. Its least-squares refinement with imposed weighted geometric constraints involving the minimization of differences in distances of chemically equivalent sets of C–C, C–N, and C–O bonds (vide supra) produced mean lengths (Table II) that are in excellent agreement with expected values.[34] The means of the two K^+–N and six K^+–O distances are within 0.02 Å of the corresponding means for the $[K(2,2,2\text{-crypt})]^+$ monocation

(34) (a) Moras, D.; Metz, B.; Weiss, R. *Acta Crystallogr., Sect. B*, **1973**, *B29*, 383–388. (b) Cisar, A.; Corbett, J. D. *Inorg. Chem.* **1977**, *16*, 632–635. (c) Cisar, A.; Corbett, J. D. *Ibid.* **1977**, *16*, 2482–2487. (d) Belin, C. H. E.; Corbett, J. D. Cisar, A. *J. Am. Chem. Soc.* **1977**, *89*, 7163–7169.

Table II. Interatomic Distances and Bond Angles for $[K(2,2,2\text{-crypt})]^+[Ni_3(\eta^5\text{-}C_5H_5)_3(\mu_3\text{-}CO)_2]^-$

	A. Intraanion Distances[a] (Å)		
Ni1–Ni2	2.442 (3)	Ni1–C11	2.195 (11)
		Ni1–C12	2.164 (12)
Ni1–Ni3	2.404 (3)	Ni1–C13	2.175 (11)
Ni2–Ni3	2.417 (3)	Ni1–C14	2.176 (11)
average	2.410	Ni1–C15	2.166 (11)
Ni3–C1	1.956 (15)	average	2.175
Ni1–C1	1.889 (15)	Ni2–C21	2.159 (10)
Ni2–C1	1.910 (15)	Ni2–C22	2.150 (9)
average	1.900	Ni2–C23	2.141 (9)
		Ni2–C24	2.146 (10)
Ni3–C2	1.916	Ni2–C25	2.157 (10)
Ni1–C2	1.944 (14)	average	2.151
Ni2–C2	1.957 (16)		
average	1.951	Ni3–C31	2.145 (10)
		Ni3–C32	2.176 (10)
C1–O1	1.210	Ni3–C33	2.179 (11)
		Ni3–C34	2.149 (10)
C2–O2	1.178	Ni3–C35	2.128 (11)
		average	2.155
		Ni1–Cp(1)[b]	1.810
		Ni2–Cp(2)	1.788
		Ni3–Cp(3)	1.796
		average	1.798
	B. Intraanion Bond Angles[a] (deg)		
Ni2–Ni3–Ni1	60.86 (8)	Ni1–C1–O1	136 (1)
		Ni2–C1–O1	133 (1)
Ni1–Ni2–Ni3	59.29 (8)	average	134
Ni2–Ni1–Ni3	59.85 (9)		
average	59.57	Ni3–C1–O1	131 (1)
Ni2–Ni1–C1	50.4 (5)	Ni1–C2–O2	132 (1)
Ni1–Ni2–C1	49.6 (5)	Ni2–C2–O2	131 (1)
average	50.1	average	132
Ni1–Ni3–C1	50.1 (5)	Ni3–C2–O2	138 (1)
Ni2–Ni3–C1	52.2 (4)		
average	51.7	Ni1–C1–Ni2	80.0 (6)
		Ni1–C1–Ni3	77.4 (6)
Ni3–Ni1–C1	52.6 (5)	Ni2–C1–Ni3	77.4 (6)
Ni3–Ni2–C1	52.2 (4)	average	77.4
average	52.4		
		Ni1–C2–Ni2	77.5 (6)
Ni2–Ni1–C2	51.5 (5)		
Ni1–Ni2–C2	51.0 (5)	Ni1–C2–Ni3	77.0 (6)
average	51.3	Ni2–C2–Ni3	77.2 (7)
		average	77.1
Ni1–Ni3–C2	52.0 (4)		
Ni2–Ni3–C2	51.0 (5)	Ni2–Ni1–Cp(1)[b]	151.8
average	50.5	Ni1–Ni2–Cp(2)	150.1
		average	151.0
Ni3–Ni1–C2	51.0 (5)		
Ni3–Ni2–C2	50.6 (5)	Ni3–Ni1–Cp(1)	148.4
average	50.8	Ni3–Ni2–Cp(2)	150.4
		average	149.0
		Ni1–Ni3–Cp(3)	147.9
		Ni2–Ni3–Cp(3)	151.3
		average	149.6
	C. Intracation Distances (Å)		
K···N1	2.979	C–C	1.521 (av 9 dist)
K···N2	2.972	C–N	1.502 (av 9 dist)
average	2.976	C–O	1.392 (av 12 dist)
K···S1(O1)	2.735	av tetrahedral angle = 110.7°	
K···S1(O2)	2.848		
K···S2(O1)	2.767		
K···S2(O2)	2.837		
K···S3(O1)	2.809		
K···S3(O2)	2.724		
average	2.787		

[a] Values for the $Ni_3(CO)_2$ core are averaged under virtual C_s-σ_v symmetry, while those involving each C_5H_5 ring are averaged under assumed C_{5v} symmetry. [b] Cp(n) denotes the centroid of the nth C_5H_5 ring.

of **2**. The near conformity of the six cryptand oxygen atoms to a trigonal prism is manifested by the average twist angle being ca. 8°.

Table III. Intramolecular Distances and Bond Angles for $Ni_3(\eta^5\text{-}C_5Me_5)_3(\mu_3\text{-}CO)_2$ (**5**) and Comparison with the $[Ni_3(\eta^5\text{-}C_5H_5)_3(\mu_3\text{-}CO)_2]^n$ Series (n = 0, (3), 1-(4))

	5 $C_{3h}-\bar{3}/m^a$ $D_{3h}-\bar{6}2m^b$	3 $C_{3h}-\bar{3}/m^a$ $D_{3h}-\bar{6}2m^b$	4 C_s-1^a C_s-m^b
	A. Distances under C_{3h} Symmetry		
Ni–Ni	[3][d]	2.530 (3)	2.389 (2)	2.421 (av)
Ni–CO	[6]	2.177 (7)	1.932 (9)	1.929 (av)
C–O	[2]	1.21 (1)	1.18 (1)	1.10 (av)
Ni–C(ring)	[15]	2.14 (av)	2.13 (av)	2.16 (av)
Ni–Cp(c)[c]	[3]	1.78	1.76	1.80 (av)
OC···CO	[1]	3.23	2.71 (3)	2.66 (av)
Ni···O	[6]	3.18	2.89 (1)	2.88 (av)
	B. Bond Angles (Deg) under C_{3h} Symmetry		
Ni–Ni–Ni	[3]	60.0	60.0	60.0 (av)
Ni–C–O	[6]	137.9 (2)	134.4 (3)	133.3 (av)
Ni–C(O)–Ni	[6]	71.1 (3)	76.4 (4)	78.3 (av)
OC–Ni–CO	[3]	95.7 (3)	88.9 (5)	87.6 (av)

[a] Crystallographic site symmetry. [b] Virtual Symmetry of $Ni_3(CO)_2$ core. [c] Cp(c) denotes the centroid of the C_5R_5 ring. [d] Brackets enclose the number of equivalent distances whose average values are listed in the right columns.

Table IV. Comparison of Selected Mean Distances and Bond Angles for the $[(\eta^5\text{-}C_5Me_5)CoNi_2(\eta^5\text{-}C_5H_5)_2(\mu_3\text{-}CO)_2]^n$ Series (n = 0 (1), 1-(2)) under Assumed C_{2v} Symmetry for the $CoNi_2(CO)_2$ Fragment

	1 (n = 0)	2 (n = 1)	difference Δ(2 - 1)
	A. Distances (Å)		
Co–Ni	[2][c]	2.371	2.391	0.020
Ni–Ni	[1]	2.326	2.388	0.062
M–M	[3]	2.356	2.390	0.034
Co–CO	[2]	1.858	1.806	−0.052
Ni–CO	[4]	2.014	1.967	−0.047
Co–C(ring)	[5]	2.074	2.100	0.026
Co–Cp(c)[b]	[1]	1.690	1.721	0.031
Ni–C(ring)	[10]	2.110	2.168	0.058
Ni–Cp(c)[b]	[2]	1.747	1.783	0.036
	B. Bond Angles (deg)		
Co–C–O	[2]	145.2	143.1	−2.1
Ni–C–O	[4]	130.5	128.3	−2.2
Co–C(O)–Ni	[4]	75.4	78.6	3.2
Ni–C(O)–Ni	[2]	70.5	74.8	4.3
OC–Co–CO	[1]	98.4	93.8	−4.6
OC–Ni–CO	[2]	88.6	84.2	−4.4

[a] Reference 10. [b] Cp(c) denotes the centroid of the C_5R_5 ring. [c] Brackets enclose the number of equivalent distances whose average values are listed in the right columns.

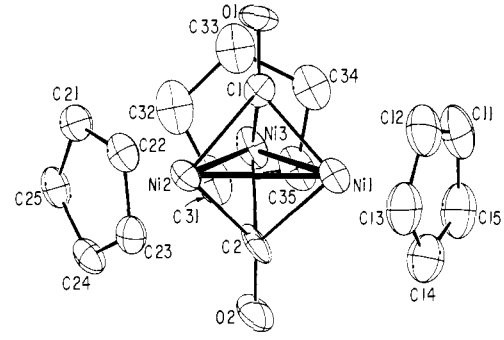

Figure 4. The diamagnetic monoanion of the neutral paramagnetic Fischer–Palm $Ni_3(\eta^5\text{-}C_5H_5)_3(\mu_3\text{-}CO)_2$ parent. The counterion is $[K(2,2,2\text{-crypt})]^+$.

The overall configuration (Figure 4) of the monoanion **4** re-

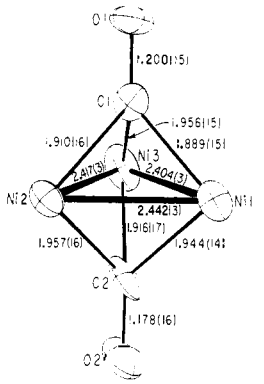

Figure 5. $Ni_3(CO)_2$ core of the $[Ni_3(\eta^5\text{-}C_5H_5)_3(\mu_3\text{-}CO)_2]^-$ monoanion, which contains two antibonding trimetal electrons, is slightly distorted from D_{3h}—$3/m2m$ symmetry toward vertical mirror-plane symmetry (C_s—σ_v).

sembles that of its neutral parent **3**. However, Figure 5, which displays the architecture of its $Ni_3(CO)_2$ core, reveals small but distinct variations of the Ni–Ni and Ni–CO bond lengths from a regular D_{3h} configuration. The three Ni–C_5H_5 (centroid) distances average 1.80 Å, while the 15 Ni–C(ring) distances average 2.16 Å.

Comparison between the Geometries of $[Ni_3(\eta^5\text{-}C_5H_5)_3(\mu_3\text{-}CO)_2]^n$ (n = 0, 1−) and Resulting Bonding Implications. The solid-state structure of the $Ni_3(CO)_2$ core in the monoanion **4** may be considered to approximate C_s—m symmetry (Figure 5), which thereby represents a geometrical distortion from the crystallographically required C_{3h}—$3/m$ site symmetry and virtual D_{3h}—$3/m2m$ symmetry of its neutral parent **3**. Nevertheless, the fact that the observed variations in **4** of its individual distances from D_{3h} symmetry are small makes it worthwhile to assume that it posseses a mean geometry of D_{3h} symmetry in order to simplify a comparative analysis of it with **3**. The following conclusions are extracted from Table III, which presents the mean bond-length data.

(a) Metal–Metal Distances. The key structural difference is that the monoanion **4** possesses an average Ni–Ni distance of 2.421 Å, which is 0.032 Å larger than that of 2.389 (2) Å in the neutral Fischer–Palm molecule **3**. This knowledge provides further proof for the trimetal antibonding character of the HOMO in **3** as the second electron is added to its to form **4**. The nondegenerate nature of the MO containing two electrons in **4** is conclusively shown from the diamagnetic character of **4** as experimentally determined by the magnetic susceptibility measurements at room temperature. These observations reinforce our previous experimental evidence[10] for the Strouse–Dahl bonding model,[12] which for the Fischer–Palm molecule **3** places the unpaired electron in the nondegenerate a_2' HOMO. It is also noteworthy that the observed average change in the three metal–metal distances is relatively constant (viz., 0.031–0.033 Å) when the Fischer–Palm molecule **3** is either reduced by one electron to **4** or formally oxidized by replacement of one nickel with a cobalt atom to give either the crystal-disordered $CoNi_2(\eta^5\text{-}C_5H_5)_3(\mu_3\text{-}CO)_2$ or the crystal-ordered $(\eta^5\text{-}C_5Me_5)CoNi_2(\eta^5\text{-}C_5H_5)_2(\mu_3\text{-}CO)_2$.

(b) Metal–Carbonyl Distances. Despite the decrease of ca. 30 cm^{-1} in the carbonyl stretching frequency upon the reduction of **3** (1742 cm^{-1}, Nujol mull) to **4** (1710 cm^{-1}, Nujol mull), there surprisingly is no statistically significant change of the mean Ni–CO bond length between **3** (with 1.932 Å) and **4** (with 1.929 Å). Nevertheless, the diminishing of the carbonyl frequency is again rationalized in terms of a charge effect, in which the additional electron in **4** pushes up the appropriate trinickel energy levels nearer the π^*(CO) levels relative to those in **3** and thereby allows for better d_π(metal) → π^*(CO) back-bonding and hence weaker C–O bonding in **4**.

(c) Metal–Cyclopentadienyl Distances. The average increase in the 15 Ni–C(ring) bond lengths by 0.035 Å on going from **3** to **4** parallels the corresponding average increase in the Ni–Ni bond lengths by 0.032 Å. It is thereby presumed that the addition of an antibonding electron to **3** to give **4** results in a "net" weakening of the Ni–C(ring) bonding. This same trend was observed upon the reduction of **1** to **2** (vide supra).

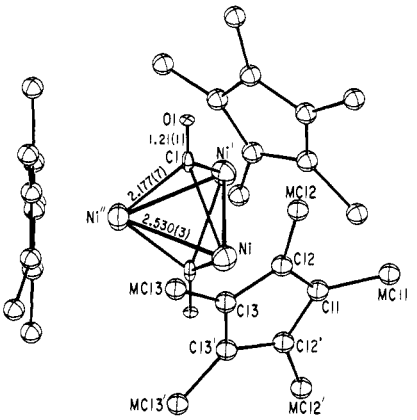

Figure 6. Permethylatedcyclopentadienyl $Ni_3(\eta^5\text{-}C_5Me_5)_3(\mu_3\text{-}CO)_2$ analogue of the Fischer–Palm $Ni_3(\eta^5\text{-}C_5H_5)_3(\mu_3\text{-}CO)_2$. This molecule of crystallographic C_{3h}—$3/m$ site symmetry for a single-crystal component of a twinned hexagonal lattice possesses a $Ni_3(CO)_2$ core of D_{3h}—$3/m2m$ symmetry. The atomic thermal ellipsoids of the C_5Me_5 rings have been idealized for the sake of clarity.

(d) Analysis of the Vertical Mirror-Plane Distortion of the $Ni_3(CO)_2$ Core of the Monoanion from D_{3h} Symmetry. The slight distortion in the $Ni_3(CO)_2$ core (Figure 5) of **4** from a regular D_{3h} configuration toward σ_v symmetry manifests itself in the appearance of two shorter Ni–Ni bond lengths of 2.404 (3) and 2.417 (3) Å and one longer Ni–Ni bond length of 2.442 (3) Å. Figure 5 also reveals that the two triply bridging carbonyl ligands are nonequivalent in their modes of asymmetrical coordination to the three nickel atoms, but yet both link each nickel atom in a compensatory bond-length fashion. One carbonyl ligand forms one longer and two shorter Ni–CO bonds, whereas the other carbonyl ligand forms one shorter and two longer Ni–CO bonds. This particular distortion, which gives rise to nearly equivalent means for the two carbonyl distances to each nickel atom, essentially preserves a balancing of the competitive π-acceptor interactions of the two bridging carbonyls with the three bonded Ni(η^5-C_5H_5) fragments. Since the *filled* nondegenerate a_2' HOMO primarily composed of antibonding trinickel orbital character cannot possess any carbonyl orbital character under threefold rotational symmetry, it is our belief that the observed distortion of **4** may possess an electronic origin (instead of being sterically induced from packing forces). The lowering of the symmetry of **4** from D_{3h} to vertical mirror-plane C_s transforms the a_2' representation of the HOMO into a a″ (that is antisymmetric with respect to the σ_v operation); the HOMO can thereby acquire carbonyl orbital character such that its charge density may be delocalized somewhat into the π^*(CO) acceptor orbitals. Although this symmetry lowering (which in general allows for greater orbital mixing) may be rationalized from energetic considerations, the observed deformation of the $Ni_3(CO)_2$ core in **4** from D_{3h} symmetry is sufficiently small that to a first approximation the HOMO may be regarded as being of a_2' representation (under assumed D_{3h} symmetry) as well as being composed largely of in-plane antibonding trinickel orbital character.

Structural Features of $Ni_3(\eta^5\text{-}C_5Me_5)_3(\mu_3\text{-}CO)_2$. *triangulo*-Tris(pentamethylcyclopentadienylnickel)dicarbonyl exists in the solid state as discrete molecules with no unusual intermolecular contacts. The molecule (**5**) has rigorous C_{3h}—$3/m$ site symmetry imposed upon it by the crystallographic twinning model (vide supra).

This cluster (Figure 6) is composed of an equilateral triangle of Ni(η^5-C_5Me_5) fragments that are linked to one another by the two triply bridging carbonyl ligands as well as by direct Ni–Ni interactions. The independent Ni–Ni distance is 2.530 (3) Å, while the independent Ni–CO and C–O lengths are 2.177 (7) and 1.21 (1) Å, respectively. Ni–C–O and Ni–C(O)–Ni bond angles are 137.9 (2)° and 71.1 (3)°, respectively.

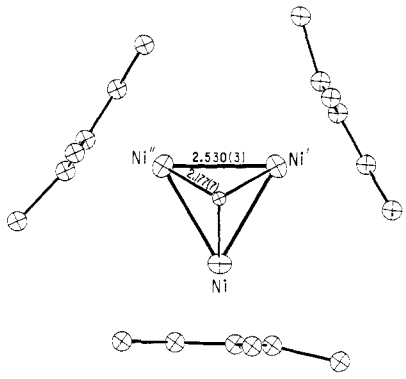

Figure 7. $Ni_3(\eta^5\text{-}C_5Me_5)_3(\mu_3\text{-}CO)_2$ of crystallographic C_{3h}—$3/m$ site symmetry viewed down the principal threefold axis. This triangular metal cluster is unprecedented (to our knowledge) in possessing three C_5Me_5 rings sterically crowded about the central $Ni_3(CO)_2$ core.

An essentially symmetrical coordination of each nickel atom to its pentamethylcyclopentadienyl ligand is indicated by the statistical equivalence of the three independent Ni–C(ring) bond lengths of 2.149 (17), 2.138 (10), and 2.118 (3) Å. The three independent C(ring)–C(ring) and three indentical C(ring)–Me bond lengths were fixed by weighted slack constraints[31] at 1.40 and 1.54 Å, respectively. The methyl carbon atom lying on the horizontal mirror plane was found to be bent out of the plane of the ring carbon atom by 9° from the nickel atom, in contrast to the corresponding bending of the other two independent methyl carbonyl atoms by less than 2°. This particular distortion is presumably due in part to steric crowding of the three bulky C_5Me_5 ligands about the $Ni_3(CO)_2$ core (Figure 7).

Structural and Electrochemical Properties of $Ni_3(\eta^5\text{-}C_5Me_5)_3(\mu_3\text{-}CO)_2$ and Resulting Bonding Conclusions Applied to the Electronically Equivalent Fischer–Palm Molecule. The important molecular parameters of the Fischer–Palm molecule **3** and its monoanion **4** together with those of the (pentamethylcyclopentadienyl)nickel carbonyl analogue **5** are presented in Table III in order to facilitate a comparative analysis. A salient structural change is the increase in **5** of the Ni–Ni distances by 0.14 Å over those in **3**. This considerable enlargement of the Ni–Ni bonds in **5** must be primarily a steric influence due to the bulky methyl substituents of the C_5Me_5 rings. The fact that the Ni–C(ring) distances of 2.135 Å (av) in **5** are analogous to (rather than larger than) those of 2.125 Å (av) in **3** emphasizes the relative weakness of the metal–metal bonds, which markedly lengthen due to steric effects in preference to an appreciable expansion of the Ni–C_5Me_5 bond lengths. In several metal–metal-bonded dimers[35] where steric effects are much less pronounced, there is only a small increase (≤0.05 Å) in the metal–metal distance upon the substitution of C_5Me_5 rings in place of the C_5H_5 rings. The similar occurrence of a 0.14-Å elongation in the two electron-pair-bonded Co–Co distances in the cubane-like $Co_4(\eta^5\text{-}C_5R_5)_4(\mu_3\text{-}P)_4$ molecule upon replacement of the cyclopentadienyl hydrogen atoms[36] by methyl substituents[37] is also ascribed to analogous intramolecular steric forces.[37]

From geometrical considerations involving angular orbital overlap, correspondingly longer Ni–CO bond lengths would have been predicted in **5** upon the lengthening of the Ni–Ni distances. However, there is no apparent explanation for the unusually long Ni–CO bond length of 2.177 (7) Å found in **5**. The fact that an infrared spectrum of **5** in cyclohexane solution exhibits a carbonyl stretching frequency of 1700 cm^{-1}, which is 42 cm^{-1} less than that in **3**, suggests a weaker C–O bond relative to that in **3**. The observed independent C–O bond length of 1.21 (1) Å in **5** is normal for a triply bridging carbonyl ligand.

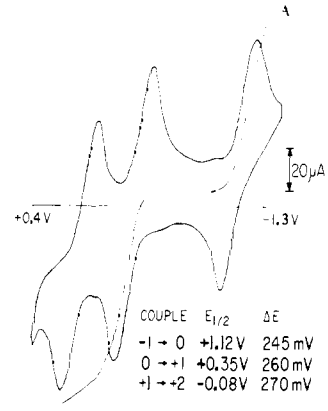

Figure 8. Cyclic voltammogram of $Ni_3(\eta^5\text{-}C_5Me_5)_3(\mu_3\text{-}CO)_2$ in THF/0.1 M $[NBu_4]^+[PF_6]^-$ at a gold disk electrode with a scan rate of 500 mV/s. $E_{1/2}$ values vs. Ag/Ag^+ electrode. Line A represents the integrated current as a function of voltage for the bulk solution.

Of interest is that the permethylated ring analogue **5** has distinctly different properties from those of **3**. Whereas **3** is greenish-black in solution, **5** is reddish-brown. A profoundly different redox behavior is exhibited by **5**. In contrast to **3** for which a cyclic voltammogram in THF solution shows only one reversible 0/−1 reduction couple at ca. −1.5 V (vs. Ag/Ag^+ reference electrode),[15] a cyclic voltammogram (Figure 8) of **5** displays, in addition to a reversible 0/−1 reduction couple at −1.21 V, two reversible +2/+1 and +1/0 reduction couples at +0.08 and −0.35 V, respectively.[38,39] Hence, unlike **3**, the neutral **5** parent apparently can be oxidized to both the monocation and dication. Efforts to isolate and crystallize salts of these charged species for structural characterization as yet have not been successful.

This capability of **5** but not **3** to exist as cationic species provides a rational justification as to why the unpaired electron in **3** cannot be removed from a highly antibonding trimetal MO but instead why this MO (which per se is destabilizing) can be populated with an additional electron in the formation of the monoanion **4**. It is apparent that these antibonding electrons provide an overall energy stabilization of the $[Ni_3(\eta^5\text{-}C_5H_5)_3(\mu_3\text{-}CO)_2]^n$ series (n = 0, 1−) simply via a charge effect. Thus, a removal of the unpaired electron by an oxidation of **3** to its unknown monocation would lead to a lowering of the nickel 3d AOs relative to the $\pi^*(CO)$ acceptor orbitals, which obviously would result in less $d\pi(Ni) \rightarrow \pi^*(CO)$ back-bonding. On the other hand, greater $d\pi(Ni) \rightarrow \pi^*(CO)$ back-bonding is achieved upon the addition of the second

(35) (a) Cirjak, L. M.; Ginsburg, R. E. Dahl, L. F. *J. Chem. Soc.*, 470–472; *Inorg. Chem.* **1982**, *21*, 940–957. (b) Curtis, M. D.; Butter, W. M. *J. Ogranomet. Chem.* **1978**, *155*, 131–145. Potenza, J. Giordano, P.; Mastropaolo, D.; Efraty, A. *Inorg. Chem.* **1974**, *13*, 2540–2544. (c) Klingler, R. J.; Butter, W.; Curtis, M. D. *J. Am. Chem. Soc.* **1978**, *100*, 5034–5038. Huang, J.-S.; Dahl, L. F., to be submitted for publication.

(36) Simon, G. L.; Dahl, L. F. *J. Am. Chem. Soc.* **1973**, *95*, 2175–2183.

(37) Johnson, R. E. Ph.D. Thesis, University of Wisconsin—Madison, 1981.

(38) For the common 0/−1 reduction couple, the electrochemical data (which indicate a more negative $E_{1/2}$ value for **3** relative to that for **5**) suggest that **5** is easier to reduce to its monoanion; this indication is contrary to the electrochemical trend found for the $(\eta^5\text{-}C_5H_{5-n}Me_n)CoNi_2(\eta^5\text{-}C_5H_5)_2(\mu_3\text{-}CO)_2$ series (n = 0, 1, 5) for which the cobalt-dinickel pentamethylcyclopentadienyl molecule (n = 5) has the highest negative $E_{1/2}$ value and hence is the most difficult one to reduce to its monoanion. In fact, for these latter compounds a relatively linear correlation was noted between the $E_{1/2}$ values and the number of methyl substituents n on the cobalt-coordinated $C_5H_{5-n}Me_n$ ring. This correlation was attributed to an additive charge-donation effect of the more electron-releasing methyl substituents, which thereby destabilizes the metal-based a_2 LUMO to which the electron is added upon formation of the monoanion. The nonapplicability of these electronic considerations to **3** vs. **5** suggests (in contrast to the three closely related $CoNi_2$ clusters) that the $E_{1/2}$ values are also being influenced by strain effects due to steric differences between the C_5H_5 and C_5Me_5 rings. In this connection, analogous steric strain arguments concerning the relative thermodynamic stability of products to reactants were utilized[39] to account for cyclic voltammetric measurements of the cubane-like $Co_4(\eta^5\text{-}C_5Me_5)_4(\mu_3\text{-}Te)_4$ and $Co_4(\eta^5\text{-}C_5H_5)_4(\mu_3\text{-}Te)_4$ molecules (which both exhibit three quasi-reversible +3/+2, +2/+1, and +1/0 reduction couples), pointing to its being more difficult to oxidize the permethylated cyclopentadienyl tetramer than the unmethylated cyclopentadienyl tetrameter to the corresponding cation.

(39) Szmanda, C. R. Ph.D. Thesis, University of Wisconsin—Madison, 1979.

antibonding electron in the reduction of **3** to **4**. These considerations emphasize that the resulting energy stabilization in the Ni–CO back-bonding due to the increased electronic charge more than compensates for the energy destabilization arising from the occupation of the trimetal antibonding HOMO by one or even two electrons.[40-42]

Acknowledgment. We are pleased to acknowledge the National Science Foundation for their support of this research. Thanks are also due to Mark H. Englert for performing magnetic susceptibility measurements and to Dr. Debasis Bhattacharya for obtaining an EPR spectrum of the cobalt–dinickel monoanion.

(40) From the experimental structured data reported herein, recent calculations[41] with the Fenske–Hall MO model,[42] which is an approximate, nonempirical procedure with the only adjustable parameters being the basis sets and molecular geometries, have substantiated our experimental quantum mechanical conclusions regarding the ground-state electronic configurations of the $[Ni_3(\eta^5\text{-}C_5H_5)_3(\mu_3\text{-}CO)_2]^n$ series ($n = 0, -1$).
(41) Rives, A. B.; You, X-Z; Fenske, R. F. *Inorg. Chem.*, in press.
(42) Hall, M. B.; Fenske, R. F. *Inorg. Chem.* **1972**, *11*, 768–775.

Registry No. 1, 77460-36-7; **2**·[K(2,2,2-crypt)]$^+$·0.5(n-C_5H_{12}), 81219-11-6; **3**, 12194-69-3; **4**·[K(2,2,2-crypt)]$^+$, 81219-12-7; **5**, 81316-26-9; $Na^+[Ni_3(\eta^5\text{-}C_5H_5)_3(\mu_3\text{-}CO)_2]^-$, 81219-13-8; $Li^+[Ni(\eta^5\text{-}C_5Me_5)(CO)]^-$, 81230-31-1; $Ni_2(\eta^5\text{-}C_5Me_5)_2(\mu_2\text{-}CO)_2$, 69239-93-6; nickelocene, 1271-28-9; $Ni(CO)_4$, 13463-39-3.

Supplementary Material Available: Six tables lising the atomic parameters and three tables giving the observed and calculated structure factor amplitudes for $[K(2,2,2\text{-crypt})]^+[(\eta^5\text{-}C_5Me_5)CoNi_2(\eta^5\text{-}C_5H_5)_2(\mu_3\text{-}CO)_2]^-\cdot 0.5(n\text{-}C_5H_{12})$, $[K(2,2,2\text{-crypt})]^+[Ni_3(\eta^5\text{-}C_5H_5)_3(\mu_3\text{-}CO)_2]^-$, and $Ni_3(\eta^5\text{-}C_5Me_5)_3(\mu_3\text{-}CO)_2$ (51 pages). Ordering information is given on any current masthead page.

Intramolecular Electron Transfer from Pentacyanoferrate(II) to Pentaamminecobalt(III): Linkage Isomers of 3- and 4-Cyanopyridine as Bridging Ligands[1]

Alek P. Szecsy and Albert Haim*

Contribution from the Department of Chemistry, State University of New York, Stony Brook, New York 11794. *Received July 13, 1981*

Abstract: The reactions of each linkage isomer of (3- and 4-cyanopyridine)pentaamminecobalt(III) with aquopentacyanoferrate(II) proceed in two stages. In the first stage, iron(II)–cobalt(III) binuclear complexes bridged by cyanopyridine are formed. The mechanism features rapid equilibration to produce an ion pair $Co(NH_3)_5L^{3+} + Fe(CN)_5OH_2^{3-} \rightleftharpoons Co(NH_3)_5L^{3+}|Fe(CN)_5OH_2^{3-}$, Q_{IP}, followed by inner-sphere substitution $Co(NH_3)_5L^{3+}|Fe(CN)_5OH_2^{3-} \rightarrow (NC)_5FeLCo(NH_3)_5$, k_f^{IP}. At 25 °C, ionic strength 0.10 M and pH 5.0, values of Q_{IP} and k_f^{IP} are in the range 447–872 M^{-1} and 13.3–42.0 s^{-1}, respectively. The second stage corresponds to the disappearance of the binuclear complexes via intramolecular electron transfer and/or back-dissociation to reactants followed by outer-sphere electron transfer. The binuclear complexes with the pyridine nitrogen bound to iron undergo intramolecular electron transfer with rate constants (25 °C, ionic strength 0.10 M) 0.16 ± 0.01 and (3.0 ± 0.2) × 10^{-3} s^{-1} for 4- and 3-cyanopyridine, respectively. The binuclear complexes with the nitrile nitrogen bound to iron undergo back-dissociation to reactants with rate constants (25 °C, ionic strength 0.10 M) 0.15 ± 0.01 and 0.46 ± 0.05 for 4- and 3-cyanopyridine, respectively. The subsequent outer-sphere electron transfer proceeds via the ion pair mechanism, the internal electron transfer rate constants within the ion pair being 0.46 and 0.71 s^{-1} for 4- and 3-cyanopyridine, respectively. The mechanisms of these and related reductions by chromium(II) and ruthenium(II) are compared and discussed.

The importance of measuring rate constants for electron-transfer reactions in the intramolecular mode has been emphasized repeatedly.[2] By exploiting the high affinity[3] of the $Fe(CN)_5^{3-}$ moiety for nitrogen heterocycles, we have been able to prepare binuclear complexes of type I simply by mixing solutions of Fe-

$$(NH_3)_5Co^{III}N\text{–}NFe^{II}(CN)_5$$
I

$(CN)_5OH_2^{3-}$ and $Co(NH_3)_5N\text{–}N^{3+}$,[4-6] where N–N represents 4,4′-bipyridine or other symmetrical bipyridines. The binuclear complexes were found to undergo intramolecular electron transfer, as well as dissociation into the reactants (eq 1 and 2, respectively).[4-6] For a series of related conjugated bridging ligands

$$(NH_3)_5Co^{III}N\text{–}NFe^{II}(CN)_5 \rightarrow (NH_3)_5Co^{II}N\text{–}NFe^{III}(CN)_5 \quad (1)$$

$$(NH_3)_5Co^{III}N\text{–}NFe^{II}(CN)_5 + H_2O \rightarrow Co^{III}(NH_3)_5N\text{–}N^{3+} + Fe^{II}(CN)_5OH_2^{3-} \quad (2)$$

containing identical donor atoms, rate constants for intramolecular electron transfer in I were found to correlate with the distance between the two metal centers.[6]

The present work was initiated in an attempt to obtain information about the effects of unsymmetrical bridging ligands on rate constants for intramolecular electron transfer. Although a fair amount of work has been done on the effects of linkage isomers on the rate constants for inner-sphere electron transfer reactions,[2,7-9] all the measurements so far have yielded second-order rate constants. Under these circumstances, the intrinsic effect of the bonding mode of the unsymmetrical ligand upon the rates of electron transfer cannot be obtained because the observed rate constants are composite quantities that include thermodynamic (equilibrium constant for formation of precursor complex) as well as kinetic (first-order rate constant for internal electron transfer) contributions. It was anticipated that, by utilizing complexes of the type $Co(NH_3)_5D\text{–}D'^{n+}$ (and their linkage isomers Co-

(1) (a) This work was supported by Grants CHE-7610449 and CHE-7909253 from the National Science Foundation. (b) Abstracted in part from the Ph.D. Dissertation of A.P.S., State University of New York, Stony Brook, NY, 1978.
(2) Haim, A. *Acc. Chem. Res.* **1975**, *8*, 264.
(3) Toma, H. E.; Malin, J. M. *Inorg. Chem.* **1973**, *12*, 1039.
(4) Gaswick, D.; Haim, A. *J. Am. Chem. Soc.* **1974**, *96*, 7845.
(5) Jwo, J.-J.; Gaus, P. L.; Haim, A. *J. Am. Chem. Soc.* **1979**, *101*, 6189.
(6) Szecsy, A. P.; Haim, A. *J. Am. Chem. Soc.* **1981**, *103*, 1679.
(7) Fay, D. D.; Sutin, N. *Inorg. Chem.* **1970**, *9*, 1291.
(8) Shea, C.; Haim, A. *Inorg. Chem.* **1973**, *12*, 3013.
(9) Balahura, R. J. *J. Am. Chem. Soc.* **1976**, *98*, 1487.

0002-7863/82/1504-3063$01.25/0